International Journal on Magnetic Particle Imaging
Vol 10, No 1, Suppl 1, Article ID 2403041, 4 Pages

Infinite Science Publishing

Proceedings Article

Simulation of a single-sided MPI handheld device with offset magnetic field for spatial encoding

Qibin Wang[a,b] · Zhonghao Zhang[a] · Lei Li[a] · Franziska Schrank[b] · Harald Radermacher[b] · Volkmar Schulz[b,*] · Shouping Zhu[a,*]

[a]School of Life Science and Technology, Xidian University & Engineering Research Center of Molecular and Neuro Imaging, Ministry of Education, Xi'an, Shaanxi 710126, China
[b]Department of Physics of Molecular Imaging Systems (PMI), Institute for Experimental Molecular Imaging (ExMI), RWTH Aachen University, Aachen, Germany
*Corresponding author, email: volkmar.schulz@pmi.rwth-aachen.de, spzhu@xidian.edu.cn

Abstract

Single-sided MPI devices provide images from regions outside of an enclosed scanner but they are constrained by limited in detection depth and non-uniform magnetic field distribution, which restrict imaging quality and sensitivity. In this study, we propose a novel handheld single-sided MPI device that utilizes an offset magnetic field with varying amplitude, coupled with high-frequency dynamic magnetic fields, to excite magnetic nanoparticles and sensitively capture the harmonic variations in spatial distribution. By moving the device horizontally in a direction perpendicular to the depth, two-dimensional spatial distribution information of magnetic nanoparticles can be acquired without the need for classical static selection fields. When the depth distance is 0-15 mm, the best spatial resolution is 1 mm. This technology holds the promise of achieving real-time imaging of superficial human tissue layers with lower cost and a simpler device structure.

I. Introduction

Magnetic nanoparticle imaging is a non-ionizing biomedical imaging modality suitable for vascular imaging, cancer screening and surgical navigation, etc.[1][2]. Single-sided MPI systems concentrate all hardware on one side of the system, providing images from regions outside of an enclosed scanner. Nevertheless, single-sided MPI systems face distinct challenges, such as limited penetration depth, difficulty in generating high-intensity selection fields[3].

To address these issues, this study proposes a method based on gradient-offset magnetic field and harmonic value encoding. Leveraging the property of magnetic field strength attenuation with distance in single-sided MPI systems, different amplitude offset magnetic fields are applied in the depth direction, coupled with high-frequency sinusoidal excitation magnetic fields to sensitize the distribution of magnetic nanoparticles within a single sampling plane[3]. By moving the device along the surface of a phantom, high-resolution two-dimensional imaging can be achieved without the use of selection fields.

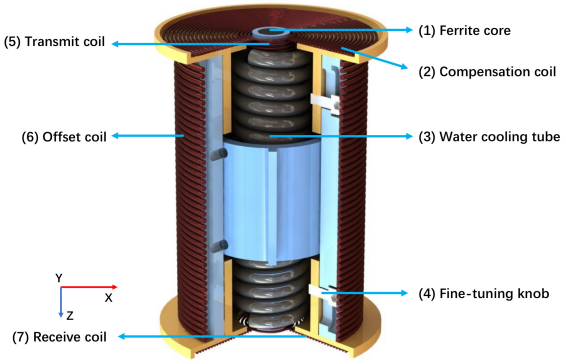

Figure 1: Schematic Diagram of device hardware composition.

Table 1: Detailed parameters of the device.

	Transmit coil	Offset coil	Receive coil and compensation coil	Ferrite core (PC40)
Inner diameter	20 mm	68 mm	22 mm	
Outer diameter	28 mm	86 mm	86 mm	20 mm
Height	120 mm	120 mm	2 mm	120 mm
Current (with ferrite)	15-60 A (AC_{peak})	0-40 A (DC)		
Current (without ferrite)	45-90 A (AC_{peak})	0-40 A (DC)		

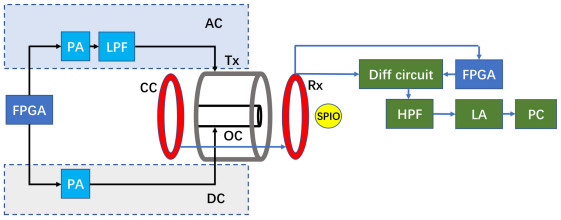

Figure 2: Signal chain diagram: PA - power amplifier, LPF - low pass filter, OC - offset coil, Rx - receive coil, CC - compensation coil, Tx - transmit coil, Diff circuit - differential circuit, HPF - high pass filter, LA - lock in amplifier, PC - computer.

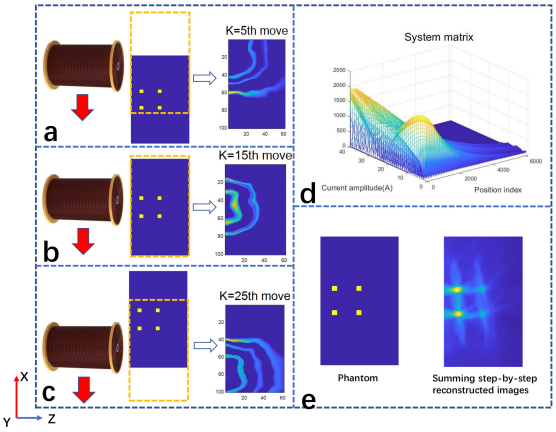

Figure 3: Fig.3a, 3b, and 3c depict the reconstructed images at the 5th, 15th, and 25th movements, respectively and the device executed a total of 34 movements. Fig.3e represents the final reconstructed image. Fig.3d represents the system matrix is constructed using the 7th harmonic.

II. Material and methods

II.I. MPI system hardware

The single-sided MPI device designed in this paper features a dual-coil structure. The outer layer comprises four layers of solid copper wire, used for generating an offset magnetic field by carrying DC current. The inner layer consists of litz wire, carrying high-frequency AC current to generate a dynamic magnetic field. At the bottom, a spiral receiving coil is designed, and at the top, a compensating coil of the same specifications as the receiving coil but wound in the opposite direction. The specific structure of the device can be seen in Figure 1, and detailed parameters are provided in Table 1.

II.II. Signal chain

The device generates a 25 kHz sinusoidal excitation signal using an FPGA, which is then applied to the transmit coil (Tx) after passing through a power amplifier (PA) and a low-pass filter (LPF). This generates an alternating magnetic field for oscillating magnetic nanoparticles within the imaging area. Simultaneously, another channel of the FPGA generates a direct current signal with varying amplitude, which, after passing through a power amplifier (PA), is applied to the offset coil (OC) to create a varying amplitude offset magnetic field.

The signals received by the receive coil (Rx) are first summed with the signals from the compensation coil (CC). After passive compensation, in the environment of zero spatial encoding, the signals are separately collected by the differential circuit and FPGA. The FPGA signal is phase calibrated to cancel the fundamental frequency component. The signals from the magnetic nanoparticles are collected through a high-pass filter (HPF), a lock-in amplifier (LA), and finally, they are input into the data acquisition card on the PC.

II.III. Simulation

The experiments in this study were exclusively conducted through simulations. The data related to the magnetic field distribution were acquired by modeling and simulating with COMSOL software, while the signal simulation of magnetic particles and the image reconstruction process were performed using MATLAB software.

10.18416/ijmpi.2024.2403041

Simulation procedure

1. Specify the scanning field of view (FOV = 50mm*30mm∧2) in the XZ plane, delineated by the blue rectangle in Figure 3. Define the sampling plane within the orange dotted box(50mm*30mm) shown in Figure 3 and establish the sampling points for the system matrix. Prescribe the direction and step size for the movement of the device, with the device's motion indicated by the red arrow in Figure 3.
2. Determine the excitation scheme, which entails maintaining a constant AC current amplitude for the transmit coil and varying the DC current amplitude of the offset coil from 0 to $I_{max} = 40$A.
3. On the marked sampling plane, using a predetermined excitation scheme, collect high harmonic information from magnetic particles at unit concentration from the specified sampling points. Construct a system matrix that relates different current values to spatial positions.
4. By moving the device within the FOV and collecting magnetic particle signals, the concentration distribution of magnetic particles within the imaging area is obtained through the solution of the system matrix, resulting in the reconstruction of a two-dimensional image.

Simulation principle In this method, owing to the abrupt changes in harmonics under different offset magnetic fields[3][4], the final two-dimensional image is reconstructed by encoding the gradient magnetic field and horizontally moving the device. The behavior of the *h-th* harmonic S_h with respect to the offset magnetic field H_{dc}, amplitude of alternating magnetic field A, T is the period and coil sensitivity σ follows Formula 1.

$$S_h = -\sigma \frac{2i}{T} M'(H_{dc}) \otimes \left(U_{h-1}(H_{dc}/A)\sqrt{1-(H_{dc}/A)^2} \right) \quad (1)$$

where U_{h-1} represents the Chebyshev polynomials of the second kind and $M'(H_{dc})$ is the derivative of the magnetic response. For single-sided MPI device, the values of the S_h, H_{dc} and σ variables change as the spatial position changes.

Constructing a system matrix using information on different current values and the positions of sampling points.

$$RX = \begin{bmatrix} S(I_1, r_1) & S(I_1, r_2) & \dots & S(I_1, r_M) \\ S(I_2, r_1) & S(I_2, r_2) & \dots & S(I_2, r_M) \\ \dots & \dots & \dots & \dots \\ S(I_N, r_1) & S(I_N, r_2) & \dots & S(I_N, r_M) \end{bmatrix} \quad (2)$$

Where RX represents the system matrix, I denotes current values, and r signifies the position index.

Correspondence of position indices:

$$r_p = Img(i, j), p = j + i*(m-1), i <= n, j <= m \quad (3)$$

where $g(i, j)$represents the position index of point p in the system matrix. n represents the number of discrete points for current values on the sampling plane, and m represents the number of discrete points in the depth direction of the sampling plane.

Using Qr represents the received signal matrix:

$$RX * C = Qr \quad (4)$$

Where C is a one-dimensional sequence representing particle concentration distribution.

Reconstruct the image:

$$\hat{U}_k = reshape(\hat{C}_k, m, n) \quad (5)$$

Where '*reshape*' is used to transform a one-dimensional sequence into two-dimensional data. Here, k denotes the image reconstructed at the k-th movement of the device, as a new image is reconstructed with each movement.

To reconstruct the image from data acquired through multiple movements of the device, the final two-dimensional reconstruction image is obtained by summing the images reconstructed step by step.

$$\hat{U} = \frac{1}{K} \sum_{k=1}^{K} \hat{U}_k(i, j - \frac{K}{2} + k) \quad (6)$$

Where K represents the number of device movements, $\hat{U}_k$signifies the position sampled after the *k-th* movement, and the reconstructed image$\hat{U}$represents the final reconstruction result. The results of stepwise reconstruction and the final reconstructed image are shown in Figure 3. The coordinate Z-axis represents depth, and the device moves in a straight line scan along the negative direction of the X-axis, moving once every 0.03 seconds.

III. Results and discussion

Figure 4a depicts the influence of the number of device movements on the quality of reconstructed images, where a single device movement corresponds to one sampling operation by default. The results indicate that as the number of device movements decreases, image quality deteriorates. To minimize the number of movements while maintaining image quality, it is advisable to have no fewer than 10 movements within a 50mm * 30mm FOV.

Figure 4b demonstrates the necessity of using different sinusoidal current values at various depth positions to achieve optimal imaging results. The red dots represent the current values that correspond to the highest imaging quality at the same depth.

10.18416/ijmpi.2024.2403041

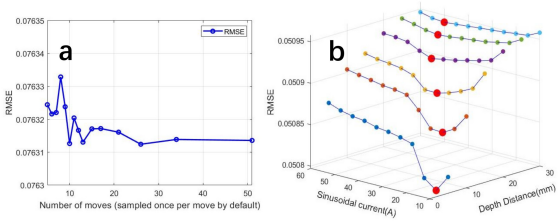

Figure 4: Fig.4a Impact of device movement count on reconstructed image quality. Fig.4b Relationship between depth distance and sinusoidal current values.

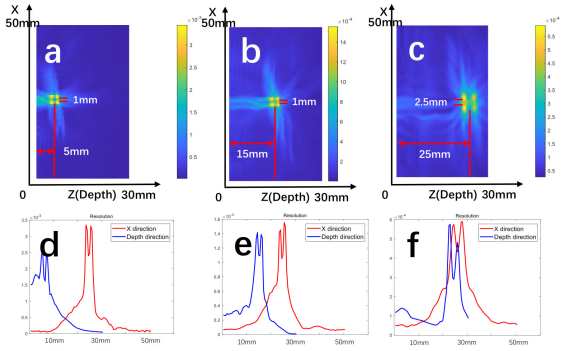

Figure 5: Best resolutions at depths of 5mm(a), 15mm(b), and 25mm(c) for the device.

By matching with the optimal sinusoidal current values, the device can achieve the highest resolution of 1mm at depths ranging from 5mm to 15mm. At a depth of 25mm, the resolution is 2.5mm, as depicted in Figure 5.

The FFL has been confirmed to exhibit higher sensitivity compared to FFP. The method proposed in this study, involving sampling across the entire plane, theoretically offers the potential for greater sensitivity. Manual mechanical scanning may cause errors in the position, and it may be necessary to mark the moving position in advance and correct the errors later. The device can operate without a ferrite core but at the cost of increased power consumption. When utilizing a ferrite core, the nonlinearity introduced by the ferrite core necessitates subsequent correction procedures.

IV. Conclusions

This study investigates the effectiveness of gradient-based magnetic field coding and the reconstruction of the system matrix reconstruction method in one-sided device mapping through simulation experiments. The best resolution within the range of 0-15mm is 1 mm and does not require the classical static selection fields. This not only reduces device size but also lowers costs, offering potential clinical value for real-time surgical navigation and imaging of superficial human tissues.

Acknowledgments

This work was supported by the National Natural Science Foundation of China under Grant Nos. 62027901, 62071362, 82272050, 61901342, the Natural Science Basic Research Program of Shaanxi Province under Grant Nos. 2021JZ-29, 2021SF-131, 2021SF-169, and the Fundamental Research Funds for the Central Universities under Grant No. JB211205

Author's statement

Conflict of interest: Authors state no conflict of interest.

References

[1] McDonough C, Pagan J, Tonyushkin A. Implementation of the surface gradiometer receive coils for the improved detection limit and sensitivity in the single-sided MPI scanner[J]. Physics in Medicine & Biology, 2022, 67(24): 245009.

[2] Gräfe K, von Gladiss A, Bringout G, et al. 2D images recorded with a single-sided magnetic particle imaging scanner[J]. IEEE transactions on medical imaging, 2015, 35(4): 1056-1065.

[3] Vogel P, Rückert M A, Friedrich B, et al. Critical Offset Magnetic PArticle SpectroScopy for rapid and highly sensitive medical point-of-care diagnostics[J]. Nature Communications, 2022, 13(1): 7230.

[4] Rahmer J, Weizenecker J, Gleich B, et al. Signal encoding in magnetic particle imaging: properties of the system function[J]. BMC medical imaging, 2009, 9: 1-21.